

Trigonal-Bipyramidal Tin(IV) Complexes Containing Tetradentate Tripodal Tristhiolatophosphine Ligands: Synthesis, Characterization, Crystal Structure, and Transmetalation Reactions

Kerry A. (Fusie) Clark and T. Adrian George*

Department of Chemistry, University of Nebraska—Lincoln, Lincoln, Nebraska 68588-0304

Received May 24, 2004

The reactions of the lithium salts of the proligands $P(C_6H_4-2-SH)_3$ ($P(HSH)_3$), $P(C_6H_3-3-SiMe_3-2-SH)_3$ ($P(TMSH)_3$), and $P(C_6H_3-5-Me-2-SH)_3$ ($P(MeSH)_3$) with $RSnCl_3$ ($R = Ph, Me, n-Bu$), in THF at 0 °C, produced a series of trigonal-bipyramidal complexes of the type $RSn(PS_3)$. The crystal structures of $PhSn(P^H S_3)$, $PhSn(P^{TMS} S_3)$, and $PhSn(P^{Me} S_3)$ reveal considerable distortion from local C_{3v} symmetry for the $Sn(PS_3)$ group. Unique to $PhSn(P^{Me} S_3)$ is the presence of intramolecular hydrogen bonding between one sulfur atom and an ortho H atom of the Ph group, creating a plane that includes this S atom and the corresponding C_6H_3 ring, a phosphorus atom, and the $PhSn$ group. An analysis of the 1H , ^{13}C , and ^{31}P NMR data from a combination of HMQC, HMBC, 2-D COSY, and $^1H\{^{31}P\}$ NMR studies reveals that in solution the $Sn(PS_3)$ groups exhibit local C_{3v} symmetry, even at low temperature. Byproducts frequently found in the synthesis of the proligands and tin complexes, and subsequent reactions, result from the oxidation of the trianionic tristhiolatophosphine ligand. The crystal structure of one of these, $[OP(HS)_2]_2$, shows that the molecule contains two ligands joined by a S–S bond. Within each original ligand the remaining two sulfur atoms form a S–S bond, and each phosphorus atom is oxidized. $PhSn(P^{TMS} S_3)$ reacted with 2 equiv of $FeCl_3$ in CH_2Cl_2 to produce the iron(IV) complex $FeCl(P^{TMS} S_3)$. $FeCl(P^{TMS} S_3)$ decomposed in the presence of excess $FeCl_3$. Similar transmetalation reactions with $FeCl_2$ or $[Fe_2OCl_6]^{2-}$ required the addition of ferrocenium ion to complete the oxidation of iron to 4+. $RuCl(P^{TMS} S_3)$ was prepared by the reaction between $PhSn(P^{TMS} S_3)$ and $RuCl_2(DMSO)_4$ without the addition of an external oxidizing agent.

Introduction

Trianionic tripodal tetradentate ligands can bind main group elements and transition metals in varying oxidation states.^{1–3} Most of the complexes have a trigonal-bipyramidal structure. For example, triamidoamine ligands with bulky or functionalized substituents on nitrogen provide steric protection for many important and unique ligands occupying the apical coordination site.^{2,4} Plass and Verkade have reported the use of the trigonal-bipyramidal azastannatranes $[Bu'Sn(MeNCH_2CH_2)_3N]$ in transmetalation reactions to form the azavanadatranes $[VO(MeNCH_2CH_2)_3N]$ and the aza-

molybdatranes $[MoN(MeNCH_2CH_2)_3N]$.⁵ Working with tripodal tristhiolatophosphine ligands of the type $[P(C_6H_4S)_3]^{3-}$, first prepared by Block, Zubieta et al.,⁶ and de Vries et al.,⁷ we have prepared and characterized novel diamagnetic iron(IV) complexes $FeX(P^{TMS} S_3)$, where $X = Cl, Br, \text{ and } I$, and $(P^{TMS} S_3)^{3-} = [P(C_6H_3-3-Me_3Si-2-S)_3]^{3-}$ (Chart 1).⁸ In a Communication,⁹ we reported the synthesis and X-ray crystal structural characterization of organotin(IV) complexes containing the tripodal tristhiolatophosphine ligands $(P^{TMS} S_3)^{3-}$, $[P(C_6H_4-2-S)_3]^{3-}$ ($(P^H S_3)^{3-}$), and $[P(C_6H_3-5-Me-2-S)_3]^{3-}$ ($(P^{Me} S_3)^{3-}$) and the transmetalation reaction of $PhSn(P^{TMS} S_3)$

* Author to whom correspondence should be addressed. E-mail: tageorge@unlserve.unl.edu.

- (1) (a) Verkade, J. G. *Coord. Chem. Rev.* **1994**, *137*, 233. (b) Verkade, J. G. *Acc. Chem. Res.* **1993**, *26*, 483.
- (2) Schrock, R. R. *Acc. Chem. Res.* **1997**, *30*, 9.
- (3) Govindaswamy, N.; Quarless, D. A., Jr.; Koch, S. A. *J. Am. Chem. Soc.* **1995**, *117*, 8468.
- (4) MacBeth, C. E.; Golombek, A. P.; Young, V. G., Jr.; Yang, C.; Kuczera, K.; Hendrich, M. P.; Borovik, A. S. *Science* **2000**, *289*, 938.

(5) Plass, W.; Verkade, J. G. *J. Am. Chem. Soc.* **1992**, *114*, 2275.

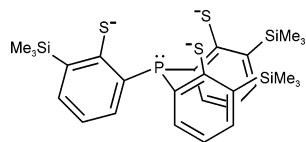
(6) Block, E.; Ofori-Okai, G.; Zubieta, J. *J. Am. Chem. Soc.* **1989**, *111*, 2327.

(7) (a) de Vries, N.; Davison, A.; Jones, A. G. *Inorg. Chim. Acta*, **1989**, *165*, 9. (b) de Vries, N.; Cook, J.; Jones, A.; Davison, A. *Inorg. Chem.* **1991**, *30*, 2662.

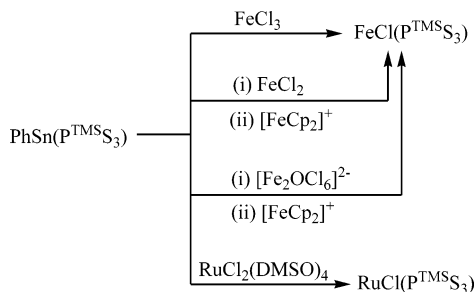
(8) Neimoth-Anderson, J. D.; Clark, K. A. (Fusie); George, T. A.; Ross, C. R., II. *J. Am. Chem. Soc.* **2000**, *122*, 3977.

(9) Clark, K. A. (Fusie); George, T. A.; Brett, T. J.; Ross, C. R., II; Shoemaker, R. K. *Inorg. Chem.* **2000**, *39*, 2252.

Chart 1



Scheme 1



with 2 equiv of FeCl_3 to produce the iron(IV) complex $\text{FeCl}(\text{P}^{\text{TMS}}\text{S}_3)$. Although tin(IV) complexes of this type are known with trianionic tripodal ligands containing a combination of one nitrogen and three sulfur atoms,^{10,11} and one phosphorus and three oxygen atoms,¹⁰ no previous examples have been reported with the soft-base combination of one phosphorus and three sulfur atoms. These complexes are phosphine analogues of thiastannatranes. In this study, we focus on (i) the synthesis of $\text{PhSn}(\text{P}^{\text{TMS}}\text{S}_3)$, $\text{PhSn}(\text{P}^{\text{Me}}\text{S}_3)$, and $\text{RSn}(\text{P}^{\text{H}}\text{S}_3)$, where $\text{R} = \text{Me}$, $n\text{-Bu}$, and Ph , and the byproducts formed, (ii) a detailed analysis of the solid-state structures and a comparison with similar trigonal-bipyramidal complexes, and (iii) transmetalation reactions that produce $\text{FeCl}(\text{P}^{\text{TMS}}\text{S}_3)$ and $\text{RuCl}(\text{P}^{\text{TMS}}\text{S}_3)$ from FeCl_2 and $[\text{Fe}_2\text{OCl}_6]^{2-}$, and $\text{RuCl}_2(\text{DMSO})_2$, respectively. The transmetalation reactions we have discovered are summarized in Scheme 1.

Experimental Section

General Procedures. All syntheses were carried out under dry nitrogen. Organic solvents were dried and purified according to standard procedures and stored under nitrogen. All solvents were bubbled with nitrogen prior to use. The ^1H , ^{13}C , ^{29}Si , and ^{31}P solution NMR spectra were recorded at 298 K on a General Electric Ω -300 NMR spectrometer (^1H , 300.52 MHz; ^{13}C , 75.57 MHz; ^{29}Si , 59.71 MHz; ^{31}P , 121.65 MHz), or at 298 or 128 K on a Bruker Ω -500 NMR spectrometer (^1H , 500.13 MHz; ^{13}C , 125.77 MHz; ^{31}P , 202.45 MHz). Chemical shifts (ppm) are reported relative to the peak for Me_4Si (^1H , ^{13}C , ^{29}Si), calculated from the chemical shifts of residual protons, and to the peak for Ph_3PO (+23.2 ppm vs 85% H_3PO_4 , 0.0 ppm), as external reference. Solid-state ^{13}C and ^{29}Si CP/MAS NMR spectra were recorded at room temperature on a Varian-100 NMR spectrometer (^{13}C , 25.03 MHz; ^{29}Si , 19.78 MHz). Chemical shifts (ppm) are reported relative to the peak for Me_4Si . The labeling within the PS_3 ligand has C1 attached to P and C2 attached to S. Mass spectra were obtained by the Midwest Center for Mass Spectrometry, Lincoln, NE. Elemental analyses were performed by Galbraith Laboratories, Knoxville, TN.

Proligands $\text{P}^{\text{H}}\text{SH}_3$ and $\text{P}^{\text{Me}}\text{SH}_3$ were prepared according to a literature procedure.⁶ The proligand $\text{P}^{\text{Me}}\text{SH}_3$ was prepared once,

using an identical procedure, starting with p -cresol. $[\text{Et}_4\text{N}]_2[\text{Fe}_2\text{OCl}_6]$ and $\text{RuCl}_2(\text{DMSO})_4$ were prepared according to reported procedures.^{12,13}

Preparation of $\text{PhSn}(\text{P}^{\text{TMS}}\text{S}_3)$. To a solution of $\text{P}(\text{TMS}\text{SH})_3$ (0.15 g, 0.26 mmol) in tetrahydrofuran (THF; 40 mL) at 0 °C was added LiBu^n (0.40 mL, 1.0 mmol in hexane). After the solution was stirred for 0.6 h, a solution of PhSnCl_3 (0.94 g, 0.31 mmol) in THF (10 mL) was added. The solution was stirred (1 h) before solvent was removed in vacuo. Methylene chloride (40 mL) was added and the resulting suspension extracted with water (3×40 mL). The yellow CH_2Cl_2 layer was separated and dried over MgSO_4 . The solution was removed by syringe and the solvent removed in vacuo. Pentane (15 mL) was added and the suspension placed in the freezer (−18 °C, 5.5 h). A cream-colored solid was collected by filtration, washed with chilled benzene (5 mL), and dried in vacuo. The yield was 75% (0.15 g, 0.20 mmol). Crystals suitable for X-ray diffraction studies were grown from a cooled (12 °C) THF–hexane (3:1 by vol) solution over 2 days. ^1H NMR (δ , CD_2Cl_2): 7.78 (td, 3H, $J = 7.75$ Hz, $J = 1.51$ Hz, 6-H, C_6H_3), 7.71 (dt, 2H, $J = 7.39$ Hz, $J = 1.25$ Hz, 2,6-H, Ph), 7.60 (dt, 3H, $J = 7.16$ Hz, $J = 1.25$ Hz, 4-H, C_6H_3), 7.53–7.47 (m, 3H, 3,4,5-H, Ph), 7.19 (td, 3H, $J = 7.39$ Hz, $J = 1.35$ Hz, 5-H, C_6H_3), 1.55 (br, H_2O), 0.423 (s, 27H, Me_3Si). ^1H NMR (δ , THF- d_8): 7.98 (ddd, 3H, $J = 7.7$ Hz, $J = 1.5$ Hz, 6-H, C_6H_3), 7.70 (dd, 2H, $J = 7.3$ Hz, $J = 1.0$ Hz, 2,6-H, Ph), 7.57 (d, 3H, $J = 7.3$ Hz, 4-H, C_6H_3), 7.48 (t, 2H, $J = 7.2$ Hz, 3,5-H, Ph), 7.43 (t, 1H, $J = 7.3$ Hz, 4-H, Ph), 7.17 (td, 3H, $J = 7.5$ Hz, $J = 1.3$ Hz, 5-H, C_6H_3), 2.92 (br, H_2O), 0.399 (s, 27H, Me_3Si). ^{13}C NMR (δ , THF- d_8): 157.27 (d, $J_{\text{CP}} = 25.8$ Hz, 2-C, C_6H_3), 148.44 (d, $J_{\text{CP}} = 29.6$ Hz, 1-C, Ph), 143.17 (d, $J_{\text{CP}} = 4.6$ Hz, 3-C, C_6H_3), 139.16 (s, 4-C, C_6H_3), 135.80 (d, $J_{\text{CP}} = 2.1$ Hz, 6-C, C_6H_3), 134.17 (s, 2,6-C, Ph), 130.92 (s, 3,5-C, Ph), 130.07 (s, 4-C, Ph), 124.92 (d, $J_{\text{CP}} = 6.2$ Hz, 5-C, C_6H_3), 123.88 (d, $J_{\text{CP}} = 73.7$ Hz, 1-C, C_6H_3), 0.043 (s, TMS). ^{31}P NMR (δ , CD_2Cl_2): −63.85 (s, $J(\text{P}^{119}\text{Sn}) = 1161$ Hz, $J(\text{P}^{117}\text{Sn}) = 1109$ Hz, $J_{\text{PC}} = 69.46$ Hz). ^{29}Si NMR (δ , CD_2Cl_2): −4.7 (d, $J_{\text{SiP}} = 4.6$ Hz). ^{29}Si CP/MAS NMR (δ): −4.6 (2), −6.3 (1). Low-resolution FABMS: m/z 768.0 $[\text{M} + \text{H}]^+$, 753.3 $[\text{M} - \text{Me}]^+$, 691.3 $[\text{M} - \text{Ph}]^+$, 359.2 $[\text{ligand}]^+$. Anal. Calcd for $\text{C}_{33}\text{H}_{41}\text{PS}_3\text{Si}_3\text{Sn} \cdot 2\text{H}_2\text{O} \cdot 0.33\text{CH}_2\text{Cl}_2$: C, 48.10; H, 5.53. Found: C, 48.07; H, 5.51.

Preparation of $\text{PhSn}(\text{PS}_3)$. This complex was synthesized in 61% yield, and diffraction-quality crystals were obtained by the procedures described above. ^1H NMR (δ , THF- d_8 /DMSO- d_6): 8.11 (t, 3H, $J = 7.75$ Hz, 6-H, C_6H_4), 7.66 (approx. d, 2H, $J = 7.15$ Hz, 2,6-H, Ph), 7.53 (t, 3H, $J = 7.75$ Hz, 4-H, C_6H_4), 7.46–7.39 (m, 3H, 3,4,5-H, Ph), 7.32 (approx. t, 3H, $J = 7.87$ Hz, 3-H, C_6H_4), 7.13 (t, 3H, $J = 7.51$ Hz, 5-H, C_6H_4). ^{13}C NMR (δ , CD_2Cl_2): 151.35 (d, $J_{\text{CP}} = 28.26$ Hz, 2-C, C_6H_4 , and/or 1-C, Ph), 135.27 (s, 3-C, C_6H_4), 134.37 (s, 2,6-C, Ph), 132.99 (s, 4-C, C_6H_4), 132.46 (d, $J_{\text{CP}} = 4.53$ Hz, 6-C, C_6H_4), 130.99 (s, 3,5-C, Ph), 130.01 (s, 4-C, Ph), 125.88 (d, $J_{\text{CP}} = 3.77$ Hz, 5-C, C_6H_4), 123.90 (d, $J_{\text{CP}} = 78.54$ Hz, 1-C, C_6H_4). ^{31}P NMR (δ , THF- d_8): −63.30 (s, $J(\text{P}^{119}\text{Sn}) = 1105$, $J(\text{P}^{117}\text{Sn}) = 1056$ Hz, $J_{\text{PC}} = 78.80$ Hz). High-resolution EIMS: m/z 551.9 $[\text{M}]^+$, 473.7 $[\text{M} - \text{Ph}]^+$. Anal. Calcd for $\text{C}_{24}\text{H}_{17}\text{PS}_3\text{Si}_3\text{Sn} \cdot 0.75\text{H}_2\text{O} \cdot 0.25\text{CH}_2\text{Cl}_2$: C, 49.70; H, 3.27. Found: C, 49.49; H, 3.26.

Preparation of $\text{PhSn}(\text{P}^{\text{Me}}\text{S}_3)$. This complex was synthesized, and diffraction-quality crystals were obtained by the procedures described above. ^{31}P NMR (δ , CD_2Cl_2): −57.99 (s, $J(\text{P}^{119}\text{Sn}) = 1127$, $J(\text{P}^{117}\text{Sn}) = 1080$ Hz).

(10) Tzschach, A.; Jurkschat, K. *Comments Inorg. Chem.* **1983**, *3*, 35.

(11) Jurkschat, K.; Mügge, C.; Tzschach, A.; Zschunke, A.; Fischer, G. *W. Z. Anorg. Allg. Chem.* **1980**, *463*, 123.

(12) Lippard, S. J.; Armstrong, W. H. *Inorg. Chem.* **1985**, *24*, 981.

(13) Evans, I. P.; Spencer, A.; Wilkinson, G. *J. Chem. Soc., Dalton Trans.* **1973**, 204.

Table 1. Summary of Crystallographic Details

	PhSn(P ^H S ₃)	PhSn(P ^{TMS} S ₃)	PhSn(P ^{Me} S ₃)	(OP ^H S ₃) ₂ ·py
empirical formula	C ₂₄ H ₁₇ PS ₃ Sn	C ₃₃ H ₄₁ PS ₃ Si ₃ Sn	C ₂₇ H ₂₃ PS ₃ Sn	C ₄₁ H ₂₉ NO ₂ P ₂ S ₆
fw	551.22	767.77	593.29	821.95
<i>T</i> (K)	293(2)	293(2)	293(2)	293(2)
wavelength (Å)	1.54178	0.71073	1.54178	0.71073
cryst syst	monoclinic	triclinic	monoclinic	monoclinic
space group	<i>P</i> 2 ₁ / <i>c</i>	<i>P</i> 1	<i>P</i> 2 ₁ / <i>c</i>	<i>P</i> 2(1)/ <i>n</i>
<i>a</i> (Å)	10.041(2)	10.111(2)	10.641(2)	9.943(2)
<i>b</i> (Å)	12.990(3)	14.737(3)	15.354(3)	13.408(3)
<i>c</i> (Å)	17.548(4)	15.342(3)	15.384(3)	28.629(6)
α (deg)	90	112.86(3)	90	90
β (deg)	96.94(3)	107.21(3)	91.85(3)	96.30(3)
γ (deg)	90	90.75(30)	90	90
<i>V</i> (Å ³)	2272.1(8)	1990.8(7)	2512.2(9)	3793.6(13)
<i>Z</i>	4	2	4	4
<i>D</i> (calcd) (Mg/cm ⁻³)	1.611	1.281	1.569	1.439
abs coeff (mm ⁻¹)	12.246	0.949	11.119	0.484
<i>F</i> (000)	1096	788	1192	1696
cryst size (mm)	0.23 × 0.12 × 0.08	0.4 × 0.4 × 0.3	0.3 × 0.3 × 0.23	0.4 × 0.3 × 0.1
θ range, deg	4.25–69.93	4.25–26.01	4.07–69.91	3.04–21.96
no. of reflns collected	5545	14905	6005	23471
no. of unique data (<i>R</i> _{int})	4296 (0.0495)	6552 (0.0391)	4757 (0.816)	4418 (0.0514)
completeness to θ, %	100.0	83.5	100.0	95.2
abs correction	Ψ scans	Ψ scans	Ψ scans	none
transm min/max	0.75/0.94			0.98/0.73
refinement method		full-matrix least-squares on <i>F</i> ²		
data/restraints/params	4296/0/262	6552/0/371	4757/0/290	4418/0/471
GOF on <i>F</i> ²	1.016	1.127	1.070	1.254
<i>R</i> 1 ^{a,c} / <i>wR</i> 2 ^{a,d}	0.0386/0.0949	0.0556/0.1418	0.0410/0.1114	0.0644/0.1553
<i>R</i> 1 ^{b,c} / <i>wR</i> 2 ^{b,d}	0.0569/0.1021	0.0681/0.1533	0.0454/0.1145	0.1011/0.1699
ρ _{max} /min (e/Å ³)	1.009/–0.545	1.226/–0.825	1.323/–2.115	0.553/–0.586

^a Denotes value for the residual considering only the reflections with *I* > 2σ(*I*). ^b Denotes value for the residual considering all the reflections. ^c *R*1 = Σ(|*F*_o – |*F*_c||)/Σ|*F*_o|. ^d *wR*2 = {Σ[w(*F*_o² – *F*_c²)²]/Σ[w(*F*_o²)²]}^{1/2}; *w* = 1/[σ²(*F*_o²) + (*aP*)² + *bP*]; *P* = [max(*F*_o² or 0) + 2(*F*_c²)]/3.

Preparation of MeSn(P^HS₃) and *n*-BuSn(P^HS₃). These complexes were synthesized by the procedures described above in 43% and 71% yields, respectively. The following are data for MeSn(P^HS₃). ³¹P NMR (δ, pyridine/CD₂Cl₂): –44.11 (s, *J*(P–¹¹⁹Sn) = 1837, *J*(P–¹¹⁷Sn) = 1756 Hz, *J*_{PC} = 77.31 Hz). Low-resolution FABMS: *m/z* 490.9 [M + H]⁺, 474.9 [M – Me]⁺, 355.0 [PS₃]⁺. The following are data for *n*-BuSn(P^HS₃). ¹H NMR (δ, CD₂Cl₂): 7.73 (t, 3H, *J* = 7.73 Hz, 6-H, C₆H₄), 7.69 (t, 3H, *J* = 7.63 Hz, 4-H, C₆H₄), 7.32 (t, 3H, *J* = 7.33 Hz, 3-H, C₆H₄), 7.16 (t, 3H, *J* = 7.51 Hz, 5-H, C₆H₄), 5.31 (s, CH₂Cl₂), 1.93–1.88 (m, 2H, 1-H, Bu), 1.81–1.71 (m, 2H, 2-H, Bu), 1.55 (b, H₂O), 1.50–1.38 (m, 2H, 3-H, Bu), 0.94 (t, 3H, *J* = 7.27 Hz, 4-H, Bu). ¹³C NMR (δ, CD₂Cl₂): 150.67 (d, *J*_{CP} = 29.94 Hz, 2-C, C₆H₄), 134.62 (s, 3-C, C₆H₄), 132.75 (s, 4-C, C₆H₄), 132.25 (d, *J*_{CP} = 7.36 Hz, 6-C, C₆H₄), 125.58 (d, *J*_{CP} = 5.98 Hz, 5-C, C₆H₄), 122.65 (d, *J*_{CP} = 71.22 Hz, 1-C, C₆H₄), 34.76 (s, 1-C, Bu), 29.02 (s, 2-C, Bu), 26.63 (s, 3-C, Bu), 14.05 (s, 4-C, Bu). ³¹P NMR (δ, CD₂Cl₂): –57.96 (s, *J*(P–¹¹⁹Sn) = 1302, *J*(P–¹¹⁷Sn) = 1245 Hz, *J*_{PC} = 75.29 Hz). Low-resolution FABMS: *m/z* 533.1 [M + H]⁺, 475.0 [M – Bu]⁺.

Transmetalation Reactions. Preparation of FeCl(P^{TMS}S₃). **Method A.** To a solution of PhSn(P^{TMS}S₃) (0.0374 g, 0.0486 mmol) dissolved in CH₂Cl₂ (30 mL) was added solid FeCl₃ (0.0129 g, 0.0795 mmol). The colorless solution turned purple very quickly. After stirring (1.5 h), the solvent was removed in vacuo. A ³¹P NMR spectrum of the purple product indicated an approximate 1:1 mixture of FeCl(P^{TMS}S₃) and PhSn(P^{TMS}S₃).

Method B. To a solution of PhSn(P^{TMS}S₃) (0.0297 g, 0.0387 mmol) dissolved in CH₂Cl₂ (30 mL) was added solid FeCl₂ (0.0082 g, 0.065 mmol). The colorless suspension was stirred (3 days), during which time the solution became green-brown. [FeCp₂][PF₆] (0.0250 g, 0.0755 mmol) was added to the solution, which turned purple during 0.5 h of stirring. The solution was extracted with water (3 × 20 mL). The CH₂Cl₂ layer was separated and dried

over MgSO₄. The purple solution was transferred to a flask and the solvent removed in vacuo. ¹H and ³¹P NMR spectra of the purple solid in CD₂Cl₂ indicated an approximate 1:2 mixture of FeCl(P^{TMS}S₃) and PhSn(P^{TMS}S₃).

Method C. To a solution of PhSn(P^{TMS}S₃) (0.0324 g, 0.0422 mmol) dissolved in CH₂Cl₂ (30 mL) was added solid [Et₄N]₂[Fe₂OCl₆] (0.00307 g, 0.0571 mmol). The gold-colored solution was stirred (2 h) until it turned green-brown, when [FeCp₂][PF₆] (0.0202 g, 0.0610 mmol) was added. The resulting purple solution was stirred for 0.5 h. The mixture was worked up as described in method B above. A ³¹P NMR spectrum of the purple solid indicated a mixture of FeCl(P^{TMS}S₃), (OP^{TMS}S₃)₂, H[(OP^{TMS}S₃)₂]⁺, and [PF₆][–].

Preparation of RuCl(P^{TMS}S₃). To a solution of PhSn(P^{TMS}S₃) (0.0319 g, 0.0415 mmol) dissolved in CH₂Cl₂ (30 mL) was added solid RuCl₂(DMSO)₄ (0.0251 g, 0.0518 mmol). During 26 h of stirring, the colorless solution turned bright amethyst. The solvent was removed in vacuo. A ³¹P NMR spectrum of the solid in CD₂Cl₂ indicated a ratio of RuCl(P^{TMS}S₃) to PhSn(P^{TMS}S₃) of 1:4. Pure amethyst RuCl(P^{TMS}S₃) was obtained by column chromatography using silica and CH₂Cl₂ as the eluent. ³¹P NMR (δ, CD₂Cl₂): 128.20 (s, *J*_{PC} = 60.2 Hz). Full characterization of this complex is reported in ref 14.

X-ray Diffraction Studies of PhSn(P^{TMS}S₃), PhSn(P^HS₃), PhSn(P^{Me}S₃), and (OP^{TMS}S₃)₂. Crystallographic details are provided in Table 1 and in the Supporting Information.

Results and Discussion

Syntheses. The proligands P(^{TMS}SH)₃ and P(^HSH)₃ were prepared by the method of Block et al.,⁶ and the ligand

- (14) (a) Clark, K. A. (Fusie). Ph.D. Dissertation, University of Nebraska—Lincoln, 2001. (b) Neimoth-Anderson, J. D.; Clark, K. A. (Fusie); George, T. A. Manuscript in preparation.

Tin(IV) Complexes Containing Trithiolatophosphine Ligands

$P(\text{MeSH})_3$ was prepared similarly starting with *p*-thiocresol.¹⁵ Chemical shift assignments in the ^1H and ^{13}C NMR spectra of $P(\text{TMS}^{\text{SH}})_3$ and $P(\text{HSH})_3$ were made using a combination of HMQC, HMBC, 2-D COSY, and $^1\text{H}\{^{31}\text{P}\}$ NMR data (Figure 1S, which is given in the Supporting Information).

The reaction of RSnCl_3 ($R = \text{Ph, Me, } n\text{-Bu}$) in THF at 0°C with the trithium salt of the ligand, prepared in situ from the thiol and *n*-BuLi (3 equiv), produced the corresponding $\text{RSn}(\text{PS}_3)$ complex (eq 1)



in greater than 60% yield, following workup of the product. The workup included a water extraction to remove salts and a pentane extraction to remove organic byproducts. A ^{31}P NMR spectrum of the pentane extract, in CD_2Cl_2 , showed a number of peaks in the 15–25 ppm region that are indicative of phosphine oxides. All attempts to prepare $\text{RSn}(\text{PS}_3)$ by the reaction of RSnCl_3 with $\text{P}(\text{SH})_3$ in the presence of NEt_3 were unsuccessful. All the tin-containing products are off-white solids that afford pale yellow solutions. Whereas $\text{PhSn}(\text{P}^{\text{TMS}}\text{S}_3)$ is soluble in all common organic solvents except aliphatic hydrocarbons, the other derivatives are only appreciably soluble in donor solvents such as THF. Heat or sonication was necessary to dissolve these latter complexes in CD_2Cl_2 for NMR studies. A detailed analysis of the ^{31}P NMR spectra of the proligands and the resulting tin complexes indicated a number of byproducts that were identified (vide infra).

Structures. X-ray analysis showed that the three phenyltin complexes possess a distorted trigonal bipyramidal structure. The atom-labeling scheme for $\text{PhSn}(\text{P}^{\text{H}}\text{S}_3)$ is given in Figure 1, and important bond lengths and bond angles for all three complexes are found in Table 2. Of the five bonds to tin, only the Sn–P distance is the same in all three structures. A comparison of the structures looking down the C–Sn–P axis is shown in Figure 2. The reverse view, looking along the P–Sn–C axis, is shown in Figure 4S, which is given in the Supporting Information.

The phenyl group on tin may adopt two distinct conformations relative to the three tin–sulfur bond vectors. In the first, the phenyl group bisects one S–Sn–S angle and eclipses the remaining Sn–S bond. To generate the second conformation, the phenyl group rotates by 90° so that it is now staggered relative to the same Sn–S bond. Inspection of Figure 2 indicates that the tin phenyl group in $\text{PhSn}(\text{P}^{\text{H}}\text{S}_3)$ and $\text{PhSn}(\text{P}^{\text{TMS}}\text{S}_3)$ adopts neither conformation. $\text{PhSn}(\text{P}^{\text{Me}}\text{S}_3)$ appears to display the eclipsed conformation. However, this may be due to apparent hydrogen bonding between S(1) and H(2)–C(2) of the tin phenyl group, $\text{S}(1)\cdots\text{H}(2) = 2.6792(11)$ Å, locking the phenyl group into this conformation. The net result of this orientation is that the phenyl, tin, phosphorus, and the corresponding *p*-tolyl groups are in the same plane. A result of this imposed orientation in $\text{PhSn}(\text{P}^{\text{Me}}\text{S}_3)$ is that the Sn–S bond lengths vary by as much as 0.128 Å and one of the S–Sn–S angles is 138° . Hydrogen bonding in

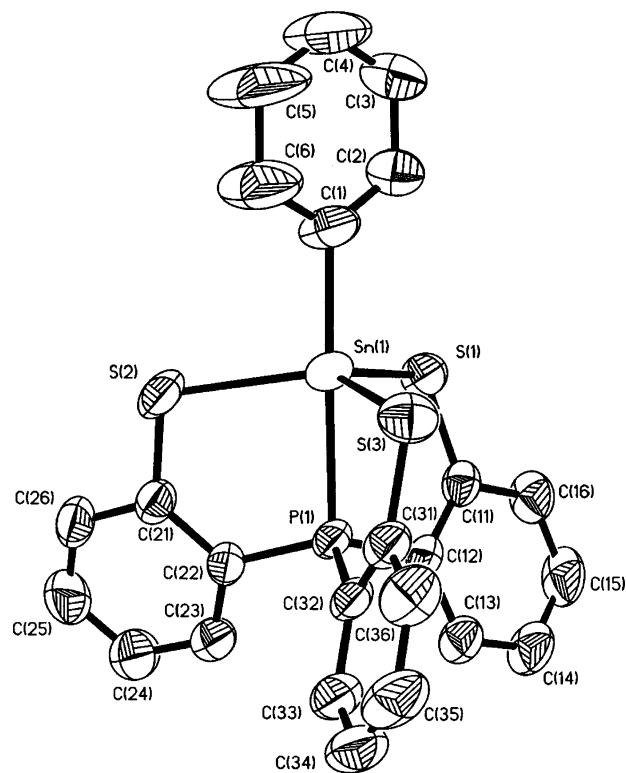


Figure 1. ORTEP plot of $\text{PhSn}(\text{P}^{\text{H}}\text{S}_3)$ showing atom labeling. Hydrogen atoms are omitted.

Table 2. Comparison of Selected Bond Lengths and Bond Angles

	$\text{PhSn}(\text{P}^{\text{H}}\text{S}_3)$	$\text{PhSn}(\text{P}^{\text{TMS}}\text{S}_3)$	$\text{PhSn}(\text{P}^{\text{Me}}\text{S}_3)$
Bond Lengths (Å)			
Sn–P	2.5161(11)	2.5132(14)	2.5124(9)
Sn–C	2.126(5)	2.175(4)	2.141(4)
Sn–S(1)	2.4972(12)	2.5093(14)	2.5120(11)
Sn–S(2)	2.4883(14)	2.5172(14)	2.5723(11)
Sn–S(3)	2.4873(14)	2.5190(13)	2.4448(11)
Bond Angles (deg)			
C–Sn–P	178.50(16)	177.12(10)	169.31(11)
S(1)–Sn–S(2)	118.57(5)	116.24(6)	137.96(4)
S(2)–Sn–S(3)	118.21(5)	119.74(5)	102.80(5)
S(1)–Sn–S(3)	117.34(5)	114.44(6)	
P–Sn–S(1)	81.66(4)	79.64(5)	81.99(3)
P–Sn–S(2)	82.09(4)	79.74(5)	77.96(3)
P–Sn–S(3)	81.09(4)	79.38(5)	85.03(3)
C–Sn–S(1)	98.71(14)	101.39(12)	94.70(12)
C–Sn–S(2)	98.97(16)	97.41(11)	98.27(11)
C–Sn–S(3)	96.66(16)	102.51(11)	105.61(11)

this complex must be due to the increased basicity of S caused by the *p*-Me group.

The $\text{Sn}(\text{PS}_3)$ moiety does not adopt C_{3v} symmetry like the $\text{M}(\text{PS}_3)$ moieties in $\text{Fe}^{\text{IV}}\text{Cl}[\text{P}(\text{C}_6\text{H}_3\text{-3-Me}_3\text{Si-2-S})_3]$ ($\text{Fe-P} = 2.157$ Å, $\text{Fe-S} = 2.108$ Å),⁸ $[\text{Fe}^{\text{II}}(\text{CO})[\text{P}(\text{C}_6\text{H}_3\text{-3-Ph-2-S})_3]]^-$ ($\text{Fe-P} = 2.165$ Å, $\text{Fe-S} = 2.290$ Å),¹⁶ $[\text{Fe}^{\text{III}}(\text{CN})[\text{P}(\text{C}_6\text{H}_4\text{-2-S})_3]]^-$ ($\text{Fe-P} = 2.141$ Å, $\text{Fe-S} = 2.167$ Å),¹⁷ and $\text{Tc}(\text{CNPr}^i)[\text{P}(\text{C}_6\text{H}_4\text{-2-S})_3]$ ($\text{Tc-P} = 2.273$ Å, $\text{Tc-S} = 2.236$ Å).^{7b} Fundamental structural differences between $\text{FeCl}(\text{P}^{\text{TMS}}\text{S}_3)$ and $\text{PhSn}(\text{P}^{\text{R}}\text{S}_3)$ are (i) the apical ligand, Cl vs Ph, (ii) an 0.357 Å increase in the metal–P distance, and (iii)

(15) $\text{P}(\text{MeSH})_3$ was first reported in Nguyen, D. H. Ph.D. Dissertation, State University of New York at Stony Brook, 1997.

(16) Nguyen, D. H.; Hsu, H.-F.; Millar, M.; Koch, S. A.; Achim, C.; Bominaar, E. L.; Münck, E. J. *Am. Chem. Soc.* **1996**, *118*, 8963.

(17) Hsu, H.-F.; Koch, S. A.; Popescu, C. V.; Münck, E. J. *Am. Chem. Soc.* **1997**, *119*, 8371.

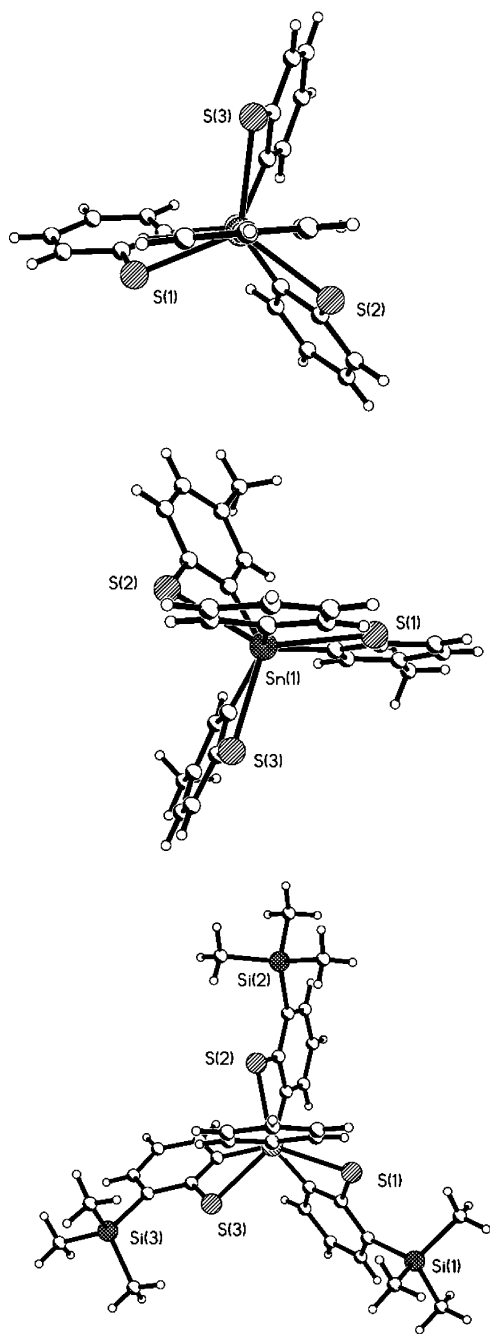


Figure 2. Comparison of the structures of $\text{PhSn}(\text{P}^{\text{Me}}\text{S}_3)$, $\text{PhSn}(\text{P}^{\text{H}}\text{S}_3)$, and $\text{PhSn}(\text{P}^{\text{TMS}}\text{S}_3)$ looking down the Ph-Sn-P axis.

an average increase of ca. 0.35 \AA in the metal–S distances. The Sn atom is displaced from the plane of S atoms, toward the phenyl group, by 0.455 [$\text{PhSn}(\text{P}^{\text{TMS}}\text{S}_3)$], 0.352 [$\text{PhSn}(\text{P}^{\text{H}}\text{S}_3)$] and 0.383 [$\text{PhSn}(\text{P}^{\text{Me}}\text{S}_3)$] \AA , respectively, compared with 0.086 \AA for Fe in $\text{FeCl}(\text{P}^{\text{TMS}}\text{S}_3)$. To accommodate the increase in the metal–sulfur distance, each sulfur atom must move away from the Sn-P axis. Each rigid, planar SC_6H_4 group is hinged at the phosphorus atom. Simply moving back the SC_6H_4 groups within each plane, to increase the metal–sulfur distance, would significantly compress the C-P-C angles and cause the three $(\text{C})\text{H}\cdots\text{H}(\text{C})$ distances to be less than the sum of the van der Waal radii (2.4 \AA). Instead, what has occurred is a simple rotation about each P-C bond, either all clockwise or all counterclockwise. This

can be seen in Figure 1, where rotation about the P-C bond of the front-facing SC_6H_4 group is clearly visible, and in Figure 4S. The C-P-C angles range from 111° to 116° in the phenyltin complexes, while the angle is 109.3° in $\text{FeCl}(\text{P}^{\text{TMS}}\text{S}_3)$. Consequences of this rotation include (i) the rotation, clockwise or counterclockwise, of the S_3 plane about the C_3 axis and (ii) the fact that the PS_3 aromatic rings are not perpendicular to the S_3 plane or parallel to the C_3 axis. Structural comparisons can only be made between $\text{PhSn}(\text{P}^{\text{H}}\text{S}_3)$ and $\text{PhSn}(\text{P}^{\text{TMS}}\text{S}_3)$ because of the hydrogen-bonding effect on the structure of $\text{PhSn}(\text{P}^{\text{Me}}\text{S}_3)$. The extent of P-C bond rotation is measured by the Sn-P-C-C torsion angles and to a lesser extent the C-Sn-S-C torsion angles (see the Supporting Information). These angles are zero in $\text{FeCl}(\text{P}^{\text{TMS}}\text{S}_3)$. Both sets of torsion angles are larger for $\text{PhSn}(\text{P}^{\text{TMS}}\text{S}_3)$ than for $\text{PhSn}(\text{P}^{\text{H}}\text{S}_3)$, ranging from 20° to 30° in the former and from 13° to 20° in the latter. A similar rotation about the axial ligand atom has been observed in trigonal-bipyramidal complexes with flexible arms such as $\text{PhSn}(\text{NHCH}_2\text{CH}_2)_3\text{N}$,¹⁸ $\text{MeSn}(\text{CH}_2\text{CH}_2\text{CH}_2)_3\text{N}$,¹⁹ and $\text{PhSi}(\text{CH}_2\text{C}_6\text{H}_2\text{-3,5-Me}_2\text{O})_3\text{N}$.²⁰ Only in $\text{PhSn}(\text{P}^{\text{H}}\text{S}_3)$ does the $\text{Sn}(\text{PS}_3)$ moiety have approximately C_3 symmetry.

Spectral Features. The room-temperature solid-state ^{13}C and ^{29}Si CP/MAS NMR spectra of $\text{PhSn}(\text{P}^{\text{TMS}}\text{S}_3)$ displayed the same lack of symmetry as found in the X-ray structure. Of 24 possible aromatic-ring ^{13}C resonances, 21 were clearly seen in the spectrum. Two broad resonances, in the ratio 2:1, were observed in the ^{29}Si NMR spectrum. Although the X-ray structure shows three different Me_3Si environments (see Figure 2), Si(1) and Si(3) are similar and sufficiently different from Si(2) to account for the 2:1 ratio.

Our initial interpretation of the solution ^1H and ^{13}C NMR data was based on the assumption that there were two possible phenyltin conformations as implied from the X-ray structures (see Figure 2). However, once the ^{13}C NMR spectra were compared at 25 and 70 MHz, it was clear that a large number of the peaks were doublets due to ^{13}C – ^{31}P coupling. In fact, phosphorus was observed to couple to all the skeletal carbon and hydrogen atoms in the PS_3 ligands in $\text{PhSn}(\text{P}^{\text{H}}\text{S}_3)$ and $\text{PhSn}(\text{P}^{\text{TMS}}\text{S}_3)$. The resonances in the room-temperature ^1H and ^{13}C NMR spectra of $\text{PhSn}(\text{P}^{\text{H}}\text{S}_3)$, $\text{PhSn}(\text{P}^{\text{TMS}}\text{S}_3)$, and $\text{BuSn}(\text{P}^{\text{H}}\text{S}_3)$ were unambiguously assigned using a combination of HMQC, HMBC, 2-D COSY, and $^1\text{H}\{^{31}\text{P}\}$ NMR data (Figure 5S, which is given in the Supporting Information). Although HMQC and HMBC spectra indicated coupling between phosphorus and all the aromatic ring carbons, in many cases the coupling constants were too small to measure in the 1D ^{13}C NMR spectra. Only two resonances were observed for the three quaternary carbons in the ^{13}C NMR spectrum of $\text{PhSn}(\text{P}^{\text{H}}\text{S}_3)$. We believe that the resonances for carbon attached to sulfur and the phenyl carbon attached to tin coincide. These carbons exhibit similar $J(\text{PC})$ values in the spectrum of $\text{PhSn}(\text{P}^{\text{TMS}}\text{S}_3)$. The

(18) Plass, W.; Verkade, J. G. *Inorg. Chem.* **1993**, *32*, 5145.

(19) Mügge, C.; Pepermans, H.; Gielen, M.; Willem, R.; Tzschach, A.; Jurkschat, K. *Z. Anorg. Allg. Chem.* **1988**, *567*, 122.

(20) Chandrasekaran, A.; Day, R. O.; Holmes, R. R. *J. Am. Chem. Soc.* **2000**, *122*, 1066.

Tin(IV) Complexes Containing Trithiolatophosphine Ligands

^{13}C chemical shifts and $J(\text{CP})$ values for the aromatic carbon atoms in the PS_3 units of $\text{PhSn}(\text{P}^{\text{H}}\text{S}_3)$, $\text{PhSn}(\text{P}^{\text{TMS}}\text{S}_3)$, $\text{BuSn}(\text{P}^{\text{H}}\text{S}_3)$, $\text{P}(\text{HSH})_3$, and $\text{P}(\text{TMSH})_3$ are compared in Table 3S, which is given in the Supporting Information. There are only six aromatic ^{13}C resonances for the PS_3 ligands of $\text{PhSn}(\text{P}^{\text{H}}\text{S}_3)$, $\text{PhSn}(\text{P}^{\text{TMS}}\text{S}_3)$, and $\text{BuSn}(\text{P}^{\text{H}}\text{S}_3)$, as found for $\text{FeCl}(\text{P}^{\text{TMS}}\text{S}_3)$. Thus, in solution the room-temperature ^{13}C NMR spectra of these complexes support C_{3v} symmetry for the $\text{Sn}(\text{PS}_3)$ moiety. Similarly, in the proton-decoupled ^{29}Si NMR solution spectrum of $\text{PhSn}(\text{P}^{\text{TMS}}\text{S}_3)$ there was only a single resonance appearing as a doublet due to coupling to phosphorus. Therefore, the solution NMR data indicate the presence of a racemic mixture of the chiral phosphine thiastrannatranes which are rapidly intraconverting at room temperature. Rapid intraconversion can be envisaged to occur by a simultaneous clockwise or counterclockwise rotation about the $\text{P}-\text{C}(12)$, $\text{P}-\text{C}(22)$, and $\text{P}-\text{C}(32)$ bonds. Similar results have been observed in trigonal-bipyramidal complexes with flexible arms such as $\text{PhSn}(\text{NHCH}_2\text{CH}_2)_3\text{N}$,¹⁸ $\text{MeSn}(\text{CH}_2\text{CH}_2\text{CH}_2)_3\text{N}$,¹⁹ and $\text{PhSi}(\text{CH}_2\text{C}_6\text{H}_2-3,5-\text{Me}_2\text{O})_3\text{N}$,²⁰ as well as the parent organic compounds bicyclo[3:3:3]undecane (manxane)²¹ and 1-azabicyclo[3:3:3]undecane (manxine).²² The presence of a single resonance for C(2) and C(6) of the phenyltin group in the ^{13}C NMR spectrum indicates rapid rotation of the phenyl group about the $\text{Sn}-\text{C}(1)$ bond in $\text{PhSn}(\text{P}^{\text{H}}\text{S}_3)$ and $\text{PhSn}(\text{P}^{\text{TMS}}\text{S}_3)$. The low-temperature (178 K) ^1H NMR spectrum showed no broadening of any signals.

The most intense peak in the FABMS of $\text{PhSn}(\text{P}^{\text{TMS}}\text{S}_3)$, $\text{BuSn}(\text{P}^{\text{H}}\text{S}_3)$, and $\text{MeSn}(\text{P}^{\text{H}}\text{S}_3)$ was due to $(\text{M} + \text{H})^+$. The former two complexes also displayed a peak due to $(\text{M})^+$. The most intense peak in the EIMS of $\text{PhSn}(\text{P}^{\text{H}}\text{S}_3)$ was due to $(\text{M})^+$. In all cases, a peak due to the loss of the apical ligand was observed. The relative isotopic intensities of these peaks agreed well with the calculated values.

Other PS_3 -Containing Products. During the synthesis of the proligands, the reaction was monitored by ^{31}P NMR spectroscopy. A number of resonances persisted that were not due to the proligand. The ^{31}P NMR spectrum of $\text{P}(\text{TMSH})_3$ occasionally displayed a pair of resonances of equal area just above the baseline at 19.0 and 3.1 ppm ($J_{\text{PP}} = 256$ Hz). An FABMS of $\text{P}(\text{TMSH})_3$ displayed, in addition to $(\text{M} + \text{H})^+$ at m/z 575.1 for $\text{P}(\text{TMSH})_3$, a peak of low intensity at $m/z = 603.0$. This peak fits a structure in which a phosphorus atom caps the ligand, $\text{P}(\text{C}_6\text{H}_3-3-\text{Me}_3\text{Si}-2-\text{S})_3\text{P}$, $\text{P}(\text{TMS}_3)\text{P}$. The unsubstituted analogue, $\text{P}(\text{H}_3\text{S})\text{P}$, was also detected in the ^{31}P NMR spectrum of $\text{P}(\text{HSH})_3$ at 15.2 and 1.7 ppm ($J_{\text{PP}} = 208$ Hz) and in the FABMS at m/z 387.0 for $(\text{M} + \text{H})^+$. Attempts were made to synthesize $\text{P}(\text{H}_3\text{S})\text{P}$ by reacting (i) $\text{PhSn}(\text{P}^{\text{H}}\text{S}_3)$ with PCl_3 in THF and (ii) $\text{P}(\text{HSH})_3$ with PCl_3 in THF. Although pure $\text{P}(\text{H}_3\text{S})\text{P}$ was not isolated from either reaction mixture, putative $\text{P}(\text{H}_3\text{S})\text{P}$ was the major product (NMR and MS data) in the latter reaction.

During an attempt to crystallize $\text{MeSn}(\text{P}^{\text{H}}\text{S}_3)$ from an acetone-pyridine solution, pale yellow crystals were col-

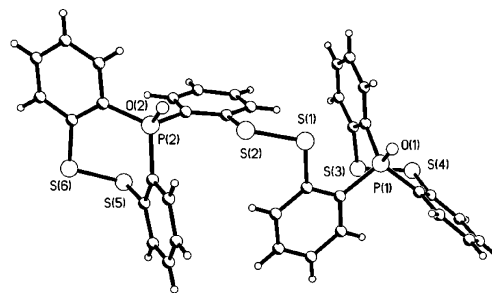


Figure 3. Ball and stick model of $(\text{OP}^{\text{H}}\text{S}_3)_2$.

lected. The crystal structure showed the complex to be an oxidized, dimerized ligand, $[(\text{C}_6\text{H}_4-\text{S}-\text{S}-2-\text{C}_6\text{H}_4)\text{P}(\text{O})(\text{C}_6\text{H}_4-2-\text{S}-\text{S}-2-\text{C}_6\text{H}_4)\text{P}(\text{O})(\text{C}_6\text{H}_4-2-\text{S}-\text{S}-2-\text{C}_6\text{H}_4)]$, $(\text{OP}^{\text{H}}\text{S}_3)_2$. The structure is shown in Figure 3. The molecule contains two ligands joined by a $\text{S}-\text{S}$ bond. The $\text{C}-\text{S}-\text{S}-\text{C}$ and $\text{C}-\text{C}-\text{S}-\text{S}$ dihedral angles of 77° and 14° (average), respectively, are similar to those found in symmetrical ortho-substituted aromatic disulfides.²³ Within each original ligand, the remaining two sulfur atoms form a $\text{S}-\text{S}$ bond and phosphorus is oxidized. The $\text{S}-\text{S}$ and $\text{C}-\text{S}$ bond lengths are statistically (5σ) the same. $(\text{OP}^{\text{H}}\text{S}_3)_2$ and the TMS analogue $(\text{OP}^{\text{TMS}}\text{S}_3)_2$ are byproducts in the synthesis of $(\text{P}^{\text{H}}\text{SH})_3$ and $(\text{P}^{\text{TMS}}\text{SH})_3$, respectively, which can be removed during proligand crystallization. The protonated form of the oxidized ligand, $\text{H}[(\text{OP}^{\text{R}}\text{S}_3)_2]^+$, was another byproduct observed in these reactions. A crystal structure of $\text{H}[(\text{OP}^{\text{TMS}}\text{S}_3)_2]^+$, as the I_3^- salt, shows the phosphine oxide groups orientated so that the oxygen atoms point toward each other.^{14b,24} In this way the hydrogen atom, which was not located, is bifurcated.

Transmetalation Reactions. The transmetalation reactions of $\text{PhSn}(\text{PS}_3)$ are summarized in Scheme 1. The slow addition of solid FeCl_3 (2 equiv) to a solution of $\text{PhSn}(\text{P}^{\text{TMS}}\text{S}_3)$ in CH_2Cl_2 resulted in the immediate formation of a purple color. Upon workup, the purple product was shown by NMR spectroscopy to be the iron(IV) complex $\text{FeCl}(\text{P}^{\text{TMS}}\text{S}_3)$ in 46% yield. An earlier preparation of $\text{FeCl}(\text{P}^{\text{TMS}}\text{S}_3)$ was carried out in three stages:⁸ (i) FeCl_2 was reacted with $\text{P}(\text{TMSH})_3$ and Et_3N (3 equiv) in MeCN to produce an emerald solution, (ii) MeCN was replaced with CH_2Cl_2 and the solution stirred until it turned brown, and (iii) ferrocenium ($[\text{FeCp}_2]^+$) hexafluorophosphate was added, which caused the color to rapidly turn purple. Following workup, $\text{FeCl}(\text{P}^{\text{TMS}}\text{S}_3)$ was isolated in about 50% yield. The first step in the FeCl_3 reaction is believed to be transmetalation (eq 3), although neither tin- nor iron-containing products were characterized. Although similar transmetalation reactions involving transfer of tetradentate tripodal ligands from tin to transition metals have been reported by Plass and Verkade,⁵ this is the first example of (i) the use of a phosphine thiastrannatranes and (ii) a transfer to iron. The second step is believed to involve facile oxidation of the putative iron(III)- $(\text{P}^{\text{TMS}}\text{S}_3)$ complex with excess FeCl_3 and

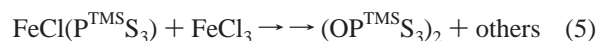
(21) Doyle, M.; Parker, W.; Gunn, P. A.; Martin, J.; MacNicol, D. D. *Tetrahedron Lett.* **1970**, 3619.

(22) Coll, J. C.; Crist, D. R.; Barrio, M. d. C. G.; Leonard, N. J. *J. Am. Chem. Soc.* **1972**, 94, 7092.

(23) Higashi, L. S.; Lundeen, M.; Seff, K. *J. Am. Chem. Soc.* **1978**, 100, 8101.

(24) Niemoth-Anderson, J. D. Ph.D. Dissertation, University of Nebraska-Lincoln, 1998.

transfer of Cl (eq 4). Alternately, iron may retain a Cl throughout the reaction. The yield of $\text{FeCl}(\text{P}^{\text{TMS}}\text{S}_3)$ was critically dependent upon the amount of FeCl_3 and the reaction time since FeCl_3 reacted with $\text{FeCl}(\text{P}^{\text{TMS}}\text{S}_3)$ to yield oxidized ligand, $(\text{OP}^{\text{TMS}}\text{S}_3)_2$ (eq 5).



For example, the reaction of FeCl_3 (1.6 equiv) and $\text{PhSn}(\text{P}^{\text{TMS}}\text{S}_3)$ for 1.5 h yielded equal amounts of $\text{FeCl}(\text{P}^{\text{TMS}}\text{S}_3)$ and unreacted $\text{PhSn}(\text{P}^{\text{TMS}}\text{S}_3)$. With 3 equiv of FeCl_3 for 1.5 h, the yield of $\text{FeCl}(\text{P}^{\text{TMS}}\text{S}_3)$ was about the same but no unreacted $\text{PhSn}(\text{P}^{\text{TMS}}\text{S}_3)$ was detected. A number of non-tin-containing phosphorus-containing complexes were produced including the oxidized ligand. When this latter reaction was stirred for 3 h, the yield of $\text{FeCl}(\text{P}^{\text{TMS}}\text{S}_3)$ was reduced considerably. With 5.8 equiv of FeCl_3 for 1.5 h, no $\text{FeCl}(\text{P}^{\text{TMS}}\text{S}_3)$ was identified, only $(\text{OP}^{\text{TMS}}\text{S}_3)_2$. Decomposition of $\text{FeCl}(\text{P}^{\text{TMS}}\text{S}_3)$ as a result of oxidation by FeCl_3 is unlikely since $\text{FeCl}(\text{P}^{\text{TMS}}\text{S}_3)$ is irreversibly oxidized in CH_2Cl_2 at 1.9 V (vs $[\text{FeCp}_2]^+/\text{FeCp}_2$, 0.0 V).⁸ $\text{FeCl}(\text{P}^{\text{TMS}}\text{S}_3)$ decomposes rapidly, to generate oxidized ligand species, in the presence of Lewis bases such as donor solvents and excess anions.^{14,24} It is the resulting six-coordinate complex that decomposes. Therefore, decomposition with FeCl_3 may occur by formation of a Lewis acid–Lewis base complex with $\text{FeCl}(\text{P}^{\text{TMS}}\text{S}_3)$ to form a six-coordinate complex such as $\text{Cl}_2\text{Fe}(\mu\text{-Cl})_2\text{Fe}(\text{P}^{\text{TMS}}\text{S}_3)$. Alternatively, FeCl_3 may remove Cl^- from $\text{FeCl}(\text{P}^{\text{TMS}}\text{S}_3)$ to form $[\text{Fe}(\text{P}^{\text{TMS}}\text{S}_3)]^+$, which is likely to be a strong enough oxidizing agent to begin oxidizing the thiolate ligand.

The reaction of $\text{PhSn}(\text{P}^{\text{H}}\text{S}_3)$ with FeCl_3 yielded no $\text{FeCl}(\text{P}^{\text{H}}\text{S}_3)$; only oxidized ligand, free proligand, and unreacted $\text{PhSn}(\text{P}^{\text{H}}\text{S}_3)$ were identified following workup. Similarly, $\text{FeCl}(\text{P}^{\text{H}}\text{S}_3)$ could not be formed by the stepwise method starting with FeCl_2 and $\text{P}^{\text{H}}\text{SH}_3$. The reaction proceeded smoothly to form putative $[\text{FeCl}(\text{P}^{\text{H}}\text{S}_3)]^-$, but oxidation by $[\text{FeCp}_2]^+$ provided only a fleeting hint of purple before decomposition occurred. Clearly, the three Me_3Si substituents play a major steric role in stabilizing $\text{FeCl}(\text{P}^{\text{TMS}}\text{S}_3)$.

The addition of solid FeCl_2 (1.5 equiv) to a solution of $\text{PhSn}(\text{P}^{\text{TMS}}\text{S}_3)$ in CH_2Cl_2 resulted in the very slow formation of a brown solution. Upon addition of $[\text{FeCp}_2]^+$ (2 equiv), the solution rapidly turned purple with the formation of $\text{FeCl}(\text{P}^{\text{TMS}}\text{S}_3)$ in 40% NMR yield. A similar reaction was carried out with 1.4 equiv of $[\text{Fe}_2\text{OCl}_6]^{2-}$, as the Et_4N^+ salt.

No $\text{FeCl}(\text{P}^{\text{TMS}}\text{S}_3)$ was identified until $[\text{FeCp}_2]^+$ was added to the solution. Oxidized ligand was also identified as a product. A similar reaction with $\text{PhSn}(\text{P}^{\text{H}}\text{S}_3)$ produced no $\text{FeCl}(\text{P}^{\text{H}}\text{S}_3)$. The only products identified were oxidized ligand and $\text{Fe}_2(\text{P}^{\text{H}}\text{S}_3)_2$. This complex is the unsubstituted analogue of $\text{Fe}_2(\text{P}^{\text{TMS}}\text{S}_3)_2$, for which the crystal structure was reported by us.⁸

The ruthenium(IV) analogue $\text{RuCl}(\text{P}^{\text{TMS}}\text{S}_3)$ was also prepared by a transmetalation reaction. Thus, the addition of solid $\text{RuCl}_2(\text{DMSO})_4$ to a solution of $\text{PhSn}(\text{P}^{\text{TMS}}\text{S}_3)$ in CH_2Cl_2 resulted in the very slow formation of an amethyst color. Following workup, $\text{RuCl}(\text{P}^{\text{TMS}}\text{S}_3)$ was isolated in 20% yield. This was higher than the yield obtained from the reaction of $\text{RuCl}_2(\text{DMSO})_4$ with $\text{P}(\text{TMS}^{\text{H}}\text{SH})_3$ and Et_3N .¹⁴ Since the reaction was carried out under anaerobic conditions, tin(IV) was the likely oxidizing agent.

Conclusions

The five-coordinate phenyltin complexes reported in this Article have distorted trigonal-bipyramidal structures with tin displaced significantly above the plane of the three equatorial sulfur atoms of the tripodal tetradentate tris-thiolatophenylphosphine ligands employed. The major cause of the upward displacement of tin is the long Sn–P bond. The other distortions are caused by the inflexibility of the ligand. However, the distorted geometry of the tin complexes may account for the facile transmetalation reactions they undergo with FeCl_3 , FeCl_2 , $[\text{Fe}_2\text{OCl}_6]^{2-}$, and $\text{RuCl}_2(\text{DMSO})_4$ to form ultimately the iron(IV) and ruthenium(IV) complexes $\text{MCl}(\text{P}^{\text{TMS}}\text{S}_3)$.

Acknowledgment. We thank the National Science Foundation for an EPSCoR Grant, the Research Corp., and the University of Nebraska Center for Materials Research and Analysis for support of this work and Dr. Joanna Clark for assistance with the crystallographic data.

Supporting Information Available: Fully labeled figures for $\text{PhSn}(\text{P}^{\text{H}}\text{S}_3)$, $\text{PhSn}(\text{P}^{\text{TMS}}\text{S}_3)$, $\text{PhSn}(\text{P}^{\text{Me}}\text{S}_3)$, and $(\text{OP}^{\text{H}}\text{S}_3)_2$; ^{13}C – ^1H HMBC spectra of $\text{P}(\text{C}_6\text{H}_4\text{-2-SH})_3$ and $\text{PhSn}(\text{P}^{\text{TMS}}\text{S}_3)$, and comparison of the structures of $\text{PhSn}(\text{P}^{\text{Me}}\text{S}_3)$, $\text{PhSn}(\text{P}^{\text{H}}\text{S}_3)$, and $\text{PhSn}(\text{P}^{\text{TMS}}\text{S}_3)$ looking down the P–Sn–Ph axis (Figures 1S, 4S, and 5S); ^{13}C chemical shifts and $J(\text{CP})$ values for the aromatic carbon atoms in the PS_3 units of $\text{PhSn}(\text{P}^{\text{H}}\text{S}_3)$, $\text{PhSn}(\text{P}^{\text{TMS}}\text{S}_3)$, $\text{BuSn}(\text{P}^{\text{H}}\text{S}_3)$, $\text{P}^{\text{H}}\text{SH}_3$, and $\text{P}(\text{TMS}^{\text{H}}\text{SH})_3$ (Table 3S); and four X-ray crystallographic files in CIF format. This material is available free of charge via the Internet at <http://pubs.acs.org>.

IC049328+